

**HIGH LEVEL EXPRESSION AND THERMAL
CHARACTERIZATION OF HUMAN CENTRIN 1**

by

Jessica M. De Orbeta Cruz

A thesis submitted in partial fulfillment of the requirements for the degree of

MASTER OF SCIENCES
in
BIOLOGY

UNIVERSITY OF PUERTO RICO
MAYAGÜEZ CAMPUS
2005

Approved by:

Nanette Diffoot - Carlo, Ph.D
Member, Graduate Committee

Date

Rafael Montalvo - Rodríguez, Ph.D
Member, Graduate Committee

Date

Belinda Pastrana - Ríos, Ph.D
President, Graduate Committee

Date

Jorge Ríos, Ph.D
Representative of Graduate Studies

Date

Lucy Williams, Ph.D
Chairperson of the Department

Date

ABSTRACT

Human centrin 1 (Hcen 1) is an acidic calcium binding protein with a molecular mass of ~ 20 kDa and has been localized in human as well as in mouse testis, at the base of the flagellar apparatus in sperm cells. Its putative function is associated with the fertilized zygote duplication and motility of the sperm. In an effort to provide a better understanding of the Hcen 1 structure, high level expression and protein purification, using affinity and anion exchange chromatography, were performed. A successful expression was obtained with optical density measures of 9 and an average of 40 grams of bacterial pellet, what leads to 10 mg of ~ 99% pure Hcen 1. Differential Scanning Calorimetry studies were done using the purified Hcen 1, obtaining two pre-transitional peaks at ~ 58.42 °C and ~ 88.82 °C. These results suggest that Hcen 1 undergoes conformational changes related with its N and C- terminal calcium binding capacities.

RESUMEN

La isoforma humana centrin 1 (Hcen 1) es una proteína ácida con capacidad para enlazar moléculas de calcio. Esta proteína tiene un peso molecular de ~ 20 kDa y ha sido localizada en el cuerpo basal del flagelo del espermatozoide. Se ha propuesto que su función esta asociada a la primera división mitótica del cigoto y al motilidad del espermatozoide. En un esfuerzo por proveer un mejor entendimiento sobre la estructura de Hcen 1 se realizaron experimentos de expresión a gran escala seguidos de dos pasos de purificación utilizando cromatografía de afinidad e intercambio iónico. Se obtuvo una densidad óptica máxima de 9 y un promedio de 40 gramos de células de bacteria, finalmente se obtuvieron 10 mg de Hcen 1 con una pureza de ~ 99%. Estudios empleando la técnica de Calorimetría Diferencial de Barrido fueron realizados utilizando muestra de la proteína purificada, dos pre transiciones fueron observadas en Hcen 1 a ~ 58.42 °C y ~ 88.82 °C, esto resultados sugieren cambios conformacionales en la proteína que podrían ser explicados por la diferencia existente en la capacidad de enlace de moléculas de calcio entre el terminal amino y carboxilo.

To my family for always being there and believe in me...

ACKNOWLEDGEMENTS

During my graduated studies I received the support and motivation of several persons. I want to express acknowledgement to my advisor, Dr. Belinda Pastrana-Rios who gave me the opportunity to research under her guidance and exceptional support. Without her support I was not be able to develop the skills necessary to become a better scientist. I also want to thank the motivation and inspiration received from Dr. Rafael Montalvo. Also, I want to thanks Dr. Nanette Diffoot for be part of my committee and for her support.

I owe special thanks to my lab family; with them this journey was more pleasant and joyful. From them I learned about science; but most important I learned about friendship. I will be always in debt with them. I am very grateful with Dr. Jeffrey Salisbury for the opportunity of researching under his supervision and with Dr. Elmar Schibel for his collaboration with this project.

The funding for this research was provided from NIH MBRS-SCORE S06GM08103.

Table of Contents

1	INTRODUCTION	1
1.1	BIOLOGICAL SIGNIFICANCE	1
1.2	OBJECTIVES	3
2	LITERATURE REVIEW.....	4
2.1	CELL CYCLE AND CENTROSOME	4
2.2	CENTRIN.....	7
2.2.1	<i>Amino Acid Sequence.....</i>	7
2.2.2	<i>Localization and Mechanism.....</i>	10
2.3	HUMAN CENTRIN 1	10
2.3.1	<i>Proposed Biological Function.....</i>	11
2.4	PROTEIN EXPRESSION.....	12
2.5	DIFFERENTIAL SCANNING CALORIMETRY.....	13
2.5.1	<i>Thermodynamic Background.....</i>	13
2.5.2	<i>Instrumentation.....</i>	15
3	MATERIALS AND METHODS	17
3.1	RECOMBINANT FULL-LENGTH HUMAN CENTRIN 1	17
3.2	EXPRESSION OF RECOMBINANT PROTEIN.....	18
3.2.1	<i>High Level Expression of Hcen 1.....</i>	18
3.2.2	<i>Biochemical Analysis.....</i>	19
3.3	PROTEIN PURIFICATION	20
3.3.1	<i>Phenyl Shepharose Chromatography.....</i>	20
3.3.2	<i>Anion Exchange Chromatography.....</i>	21
3.3.3	<i>Protein Characterization.....</i>	21
3.4	CALORIMETRIC STUDIES.....	22
3.4.1	<i>Sample Preparation</i>	22
3.4.2	<i>DSC Procedure.....</i>	22
4	RESULTS AND DISCUSSION	24
4.1	PROTEIN EXPRESSION AND PURIFICATION	24
4.2	DIFFERENTIAL SCANNING CALORIMETRY.....	34
5	CONCLUSIONS AND FUTURE WORK.....	38

Table List

TABLE 1. SUMMARY OF AMINO ACID SEQUENCE RESULTS..... 24

Figure List

FIGURE 1. REPRESENTATION OF THE LOCI OF HUMAN CENTRIN ISOFORMS IN HUMAN CHROMOSOMES	2
FIGURE 2. THE DIAGRAM ABOVE SHOWS THE COORDINATION BETWEEN THE CELL AND CENTRIOLE CYCLES. IN G ₁	7
FIGURE 3. EVOLUTIONARY TRACE AND STRUCTURAL HOMOLOGY FOR CALMODULIN, TROPONIN C AND CENTRIN.	9
FIGURE 4. DIAGRAM OF A DIFFERENTIAL SCANNING CALORIMETER USED FORM THERMAL STUDIES.	16
FIGURE 5. MAP OF pT7-7 VECTOR USED TO EXPRESS HCEN 1.	18
FIGURE 6. GROWTH CURVE FOR <i>E. COLI</i> TRANSFORMED WITH pT7-7 DURING IPTG INDUCTION FOR HCEN 1 EXPRESSION.	25
FIGURE 7. GROWTH CURVE FOR <i>E. COLI</i> TRANSFORMED WITH pT7-7 DURING IPTG INDUCTION FOR ¹³ C- HCEN 1 LABELED.	26
FIGURE 8. TIME COURSE OF HIGH LEVEL EXPRESSION OF HCEN 1.	26
FIGURE 9. SDS-PAGE FOR THE BACTERIAL PELLET LYSATE AFTER HIGH LEVEL EXPRESSION.	28
FIGURE 10. ELUTION PROFILE CHARACTERISTIC OF HCEN 1 TROUGH AFFINITY CHROMATOGRAPHY.	29
FIGURE 11. SDS-PAGE FOR THE FRACTION ELUTED AFTER AFFINITY CHROMATOGRAPHY.	29
FIGURE 12. BRADFORD ANALYSIS OF THE FRACTIONS ELUTED FROM THE AFFINITY COLUMN.	30
FIGURE 13. ELUTION PROFILE CHARACTERISTIC OF HCEN 1 TROUGH ANION EXCHANGE CHROMATOGRAPHY.	31
FIGURE 14. SDS-PAGE FOR THE FRACTION ELUTED AFTER AFFINITY CHROMATOGRAPHY.	32
FIGURE 15. CHARACTERISTIC UV SPECTRA FOR HCEN 1.	33
FIGURE 16. MALDI MASS SPEC FOR HCEN 1.	33
FIGURE 17. MALDI MASS SPEC FOR ¹³ C- HCEN 1.	34
FIGURE 18. THERMOGRAM FOR HCEN1 AT 20 mM.	36
FIGURE 19. THERMOGRAM OF HCEN1 AT 40 mM.	36
FIGURE 20. THERMOGRAM OF HCEN1 AT 60 mM.	37

1 INTRODUCTION

1.1 Biological Significance

Among the cell components the microtubules are one of the most studied but, in spite of this, its functions and characteristics are still not well understood. This cell component is characterized by a microtubule organizing center (MTOC) which usually establishes the number, direction and polarity of the microtubules (Moudjou et al., 1991). In mammalian cells the MTOC is the centrosome. The proteins associated with centrosomes are commonly conserved among phylogenetic related organism, but proteins as γ tubulin and recently, centrin has been found conserved in a diverse group (Weich et al. 1996).

Centrin is an acidic calcium binding protein with a molecular mass of ~ 20 kDa. This protein was first studied in flagellated organism, as the algae *Chlamydomonas reinhardtii* (Salisbury et al., 1984). In the algae, the protein was identified as a mayor component of the basal body associated with the contractile striated flagellar roots (Baron et al., 1995). Centrin was found later as a component of centrosome and mitotic spindle in higher eukaryotes. The cDNA clones from yeast to human encoding centrin, have been isolated and sequenced. Its amino acid sequence reveals that centrin is a highly conserved protein (Salisbury 1995; Salisbury 1998).

In *Homo sapiens* three genes that encode for centrin have been identified (Figure 1). These genes are located on chromosome 18 designated as *cen1*, chromosome X designated as *cen2* and 5 designated as *cen3* (Salisbury 1995). The presence of Human centrin 1 (Hcen 1) has been demonstrated in human as well as in mouse testis, at the base

of the flagellar apparatus in sperm cells and its putative function is associated with the fertilized zygote duplication and motility of the sperm (Errabolu et al., 1994).

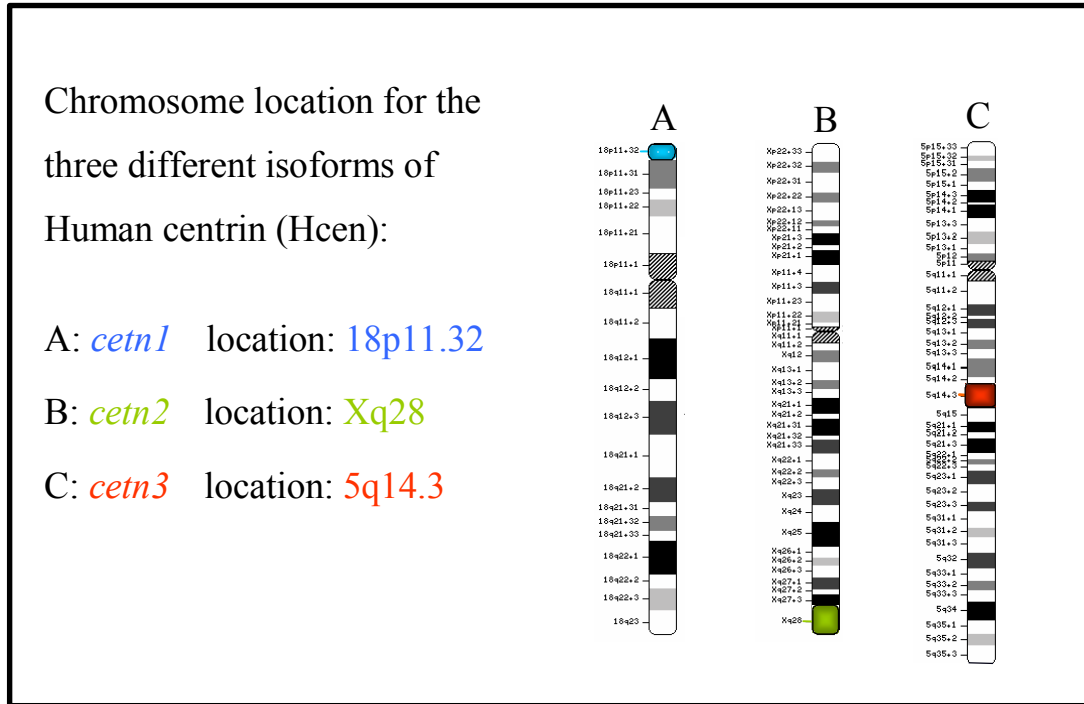


Figure 1. Representation of the loci of Human centrin isoforms in human chromosomes. Information modified from the National Center for Biotechnology Information, Map Viewer.

1.2 Objectives

In order to provide more information about Hcen 1 structure and function we propose to perform thermal dependence studies using Differential Scanning Microcalorimetry. These experiments can lead to a better understanding of Hcen 1 stability and can be used as reference for further biophysical studies such infrared spectroscopy and circular dichroism. In our research we propose to use high level bacterial expression of centrin and its subsequent purification to obtain the sufficient protein necessary to perform future biophysical studies.

2 Literature Review

2.1 Cell Cycle and Centrosome

In eukaryotic cells the number, direction and polarity of microtubules is organized by the microtubule organizing center (MTOC). This organization center differs in appearance from species to species. In mammalian cells the organization center is the centrosome, which comprises a pair of centrioles surrounded by the pericentriolar material. The centrosome functional significance has been demonstrated by microsurgical removal and the knock down technique, which leads to uncouple cell growth (Moudjou et al., 1991). Once during each cell cycle the centrosome doubles from one to two in a process that is initiated by centriole duplication. Centrosome increase in size through the recruitment of pericentriolar material, and the two centrosomes of G₂/M cells show a dramatic increase in microtubule nucleating activity (Palermo et al., 1997).

The control of centrosome duplication and their capacity to nucleate microtubules is tightly coupled to cell cycle progression largely through the action of G₁/S and G₂/M cell cycle regulators. The coupling of the cell cycle and centrosome duplication have been describe in detail by Salisbury (2001); after the cell undergoes mitosis the centrioles change their arrangement (Figure 2). They are oriented with the proximal end of the of the daughter centriole positioned along the lateral proximal wall of the mature centriole such that the two centrioles are in orthogonal arrangement, this occurs during G₁ phase. Once the cell pass the G₁ restriction point and commit to S phase DNA replication, the two centrioles separate a short distance from one another and procentrioles begin to form

along the lateral wall of the proximal end of each existing centriole. The characteristic arrangement seen for procentriole formation as well as clues from the yeast SPB duplication process suggests that centriole biogenesis is a template driving process.

During G₂ phase the newly forming centrioles elongate and the pre-existing daughter centriole acquires molecular and structural features characteristic of a mature centriole including acquisition of a halo-pericentriolar material and its associated microtubule nucleation capacity (Chang and Stearns, 2000; Piel et al., 2000). Thus, during G₂/M, three generations of centrioles are present in the same somatic cell: the mature centriole, the daughter centriole and the two nascent centrioles. At the G₂/M cell cycle transition the two pairs of centrioles migrate to opposite sides of the prophase nucleus and serve as the mitotic spindle poles. Thus, the centrosome is duplicated only once during a normal cell cycle to give rise to two centrosome that function as the spindle poles of the dividing cell (Salisbury 2001).

Abnormal duplication of centrosome has been implicated as causes of chromosome instability and defects, characteristics of certain types of tumors (Lingle et al., 1998). In breast tumors tissue architecture is highly disrupted, especially in those components regarding cell polarity (Lutz et al., 2001). Staining of breast tumors with antibodies against centrosome proteins; as centrin, pericentrin and γ tubulin have confirmed abnormalities in the cell (Carroll et al., 1999). Subsequent studies of breast tumor tissue using electron microscopy have revealed an increasing in centrosome number and volume, accumulation of pericentriolar material and cells with multiple centrioles (Lingle et al. 1998). The protein p53, cyclins/cdk and human centrin are

among the proteins involved in the development of centrosome defects in human breast tumors (Carroll et al. 1999).

Previous studies using MCF-7, vMCF-7^{DNp53} and MDA-MB 231 cells, treated with hydroxyl urea, have suggest that p53 and cyclin/cdk may regulate centrosome homeostasis maintaining the integrity of the G₁/S cell cycle checkpoint (D'Assoro et al., 2004) following genotoxic stress. Preliminary studies with the MCF-7 cells treated with tamoxifen, an anticancer therapeutic drug, have also been carried (Appendix 1). The treatment was applied to the cells in order to provide information of how established chemotherapeutic drug may act on the cells and to have a better understanding of the relation of G₁/S check point function and relation with centrosome cycle. After hormone starvation and addition of tamoxifen a delayed on cyclins E and D was observed, while cyclins A and B appeared at the same time in both treated and untreated cells (*unpubl. data*).

The expression of centrin was also verified and was constant in tamoxifen treated cells. According with the cell cycle and centrosome cycle coupling the expression of centrin should be increasing 4 hours after the hormone addition and began to decrease at 24 hours. These results may suggest that tamoxifen is causing cell cycle deregulation that is overcome due to the expression of cyclins A and B and that the cell cycle is uncouple with the centrosome cycle. The uncoupling between the two cycles may cause centrosome duplication that can lead to chromosome instability even in cells treated with chemotherapeutic drugs.

The centrosome is a key component to maintain cell stability. Structural defects in it have been identified as possible causes of chromosomal instability and tumor

progression. While its relation with cell cycle progression and coupling has been established, its composition remains unclear and poorly understood (Kalt and Schliwa, 1993). A better understanding of the proteins that forms part of the centrosome and how these proteins interact with other cell cycle regulators might be the key to understand the interplay of centrosome and cell cycle.

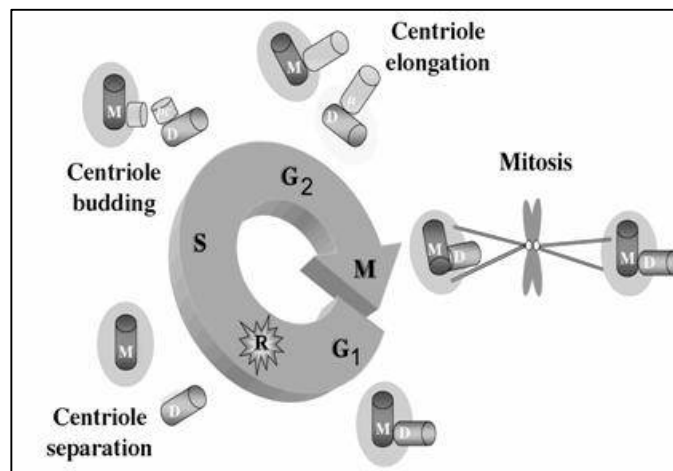


Figure 2. The diagram above shows the coordination between the cell and centriole cycles. In G₁ the pair of centrioles are labeled: M represents the mature centriole surrounded by pericentriolar material and D represents the daughter centriole. They are arranged in the characteristic orthogonal orientation. As the cell cycle progress they separate from each other and duplication begins in S phase. Later in S phase the procentriole assembles near the proximal end of each pre- existing centriole and during G₂ the procentriole elongate. Once the cell enters mitosis the two pairs of centrioles move to opposite sides of the nucleus. (Reprinted from Salisbury 2001)

2.2 Centrin

2.2.1 Amino Acid Sequence

Although, centrosome related structures may conserve a similar function in different species the specific components were conserved phylogenetically, with some

exceptions. The centrosomal proteins γ tubulin and centrin are present in a variety of species including yeast, algae and humans (Oakley and Oakley, 1989; Weich et al., 1996). Centrin is a calcium binding protein, as are calmodulin, troponin C and parvalbumin. It was first discovered in the green algae *Tetraselmis striata* as a component of the striated flagellar root (Salisbury et al., 1984). This calcium modulated protein is thought to be arisen within the ancestor of all eukaryotes *via* gene duplication (Hart et al., 1999).

Centrins are classified in the EF-hand subfamily within the superfamily of the calcium modulated proteins. The basic EF-hand domain consists of two perpendicular 10 to 12 residue alpha helices with a 12-residue loop region between, forming a single calcium-binding site, which give the characteristic conformation of helix-loop-helix (Henikoff et al., 1997). Calcium ions interact with residues contained within the loop region. Each of the 6 residues in the loop region is important for calcium coordination. In EF-hand domains, residues 1, 3, 5, 7, 9, and 12 of the conserved loop region provide oxygen ligands to the calcium ion necessary for its binding (Kuboniwa et al., 1995).

A remarkable characteristic of the calcium modulated superfamily is its structural homology and as in proteins as calmodulin and troponin C a highly conservation of the EF-hand domain can be found in centrin (Battacharya et al., 1993). Amino acid analysis reveals that centrin is a highly conserved protein, among vertebrates centrin amino acid sequence is 80-90% conserved and for lower organism is conserved in a 50-70% (Figure 3). The mayor difference in this protein among organisms is its amino terminal sequence what becomes to be most divergent part of the sequence between species (Lee and Huang, 1993; Errabolu et al., 1994).

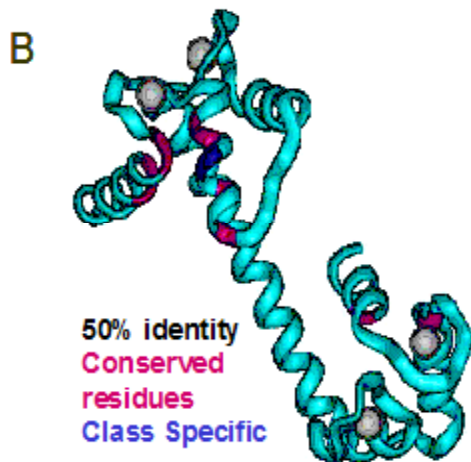
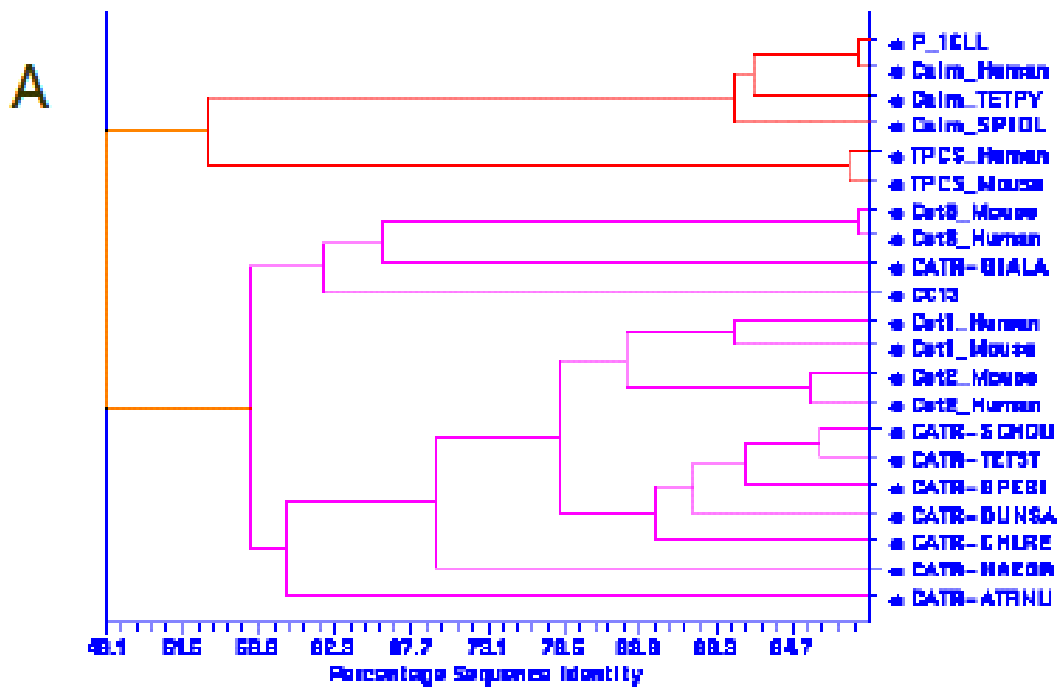


Figure 3. (A) Evolutionary trace and (B) structural homology for calmodulin, troponin C and centrin; created using NCBI-BLAST, ClustalW and Insight II from Accelrys. (Reprinted from Ortiz et al. 2004)

2.2.2 Localization and Mechanism

Centrin has been extensively studied in green algae such as *Chlamydomonas reinhardtii* and *Scherffelia dubia*. In these organisms centrin participates in the contraction of fibers of the nucleus-basal body connectors and of the fibers interconnecting the basal bodies (Schiebel and Bornes, 1995). The centrin contraction mechanism observed results are different from the sliding filament of muscle contraction. Fibers containing centrin twist and supercoil; forming an electron-dense globule as they contract (Sanders et al., 1989). The contraction or shortening of the fibers could occur even in the absence of ATP, but exclusively attributed to Ca²⁺ binding (Finst et al., 1998).

A phenotype of the mutant *vfl2*, that contains a point mutation in centrin structural gene, in *Chlamydomonas* revealed important functions within the nucleus-basal body apparatus. In the alga, this mutation causes a variable number of flagella and abnormal positioning of the basal bodies in the cell. The aberrant positing of the basal bodies suggests that centrin could be related to the duplication of this organelle (Spang et al., 1993). Centrins' homologue in yeast, CDC31, has been demonstrated to be essential in the assembly of the spindle pole body (SPB). In *S. cerevisiae* a temperature sensitive mutant of CDC31 demonstrated it to be unable to complete the first step of the SPB duplication, an important step for cell division in yeast (Spang et al., 1993).

2.3 Human centrin 1

Human centrins, are approximately 84% conserved. These centrin isoforms are comprised of 172 amino acids, with only 28 point differences within its sequence and 12

of these occur in the amino terminal domain, being this region, the most divergent. Other important characteristic, reported Hcen 1 and Hcen 2, have bind to only two Ca^{+2} ions while having four binding sites, in contrast with proteins from lower organism that can bind four Ca^{+2} ions per molecule. While, Hcen2 and Hcen3 are related with the centrosome and pericentriolar material respectively, Hcen1 has been detected only in basal body of the human sperm flagella (Errabolu et al. 1994)

In mouse as in humans three centrin genes have been identified and their locations are similar to the ones determined before for humans, due to this mouse has become a model for the study of centrin function in mammals (Hart et al., 1999; Salisbury et al., 2001). A work using the mouse centrin 1 gene, analyzed with respect to its chromosome structure and tissue expression results in the possibility that centrin 1 could be an expressed retroposon. The expression of centrin 1 using mRNA has been tested in a variety of tissues including kidney, brain, spleen, skeletal muscle, testis, ovary and oviduct; resulting expression only in the testis (Hart et al., 1999).

2.3.1 Proposed Biological Function

Different from somatic cells, where the chromosomes simply duplicate, in gametic cells only half of the chromosomes should be present in order to ensure normal fertilization. The structure responsible for the organized distribution of the genetic material is the mitotic spindle, which is generated from the centrosome. In human oocytes there an apparent lack of centriolar structure, while in human sperm the presence of these structure has been proved (Sathanathan et al., 1991). If both gametic cells retain

their centrosomes and remained functional the zygote would enter its first division with a duplication of the centrosome, what leads to abnormal multipolar cells resulting in aberrant cell division (Sathanathan et al., 1996).

To avoid centrosome duplicity one of the gametes is down regulated and in most species is the spermatozoon that introduce the functional centrosome (Schatten, 1994). Thus suggesting that Human centrin 1, once fertilization occurs, is responsible for the first zygote division. To verify the relation between Hcen 1 and the centrosome in gametic cells the mouse has been used as a model, since mouse centrin genes are very similar to *Homo sapiens*. The developmental expression of mouse centrin1 in the testis is only detected after 14 days post partum, period that correspond to the first spermatogenesis, characterized by the previous acquisition of meiotic competence (Manandhar et al., 1999). The ability to undergo meiosis is an event preceded by the inactivation of the X chromosome. An inactivation of the X chromosome may suggest that the origin of centrin 1 gene could be a compensatory mechanism; that replaces in certain way the reduction of centrin 2 expression when the single X chromosome of the male is inactivated (Hart et al., 1999). This suggests that Hcen 1 may have an important role during the first zygote division.

2.4 Protein Expression

Large scale culture of recombinant *Escherichia coli* strains are used commercially in the manufacture of several peptide products, but there is no formal or universal fermentation process for expression of all recombinant proteins (Wood and Komives, 1999). The levels of foreign gene expression in *E. coli* are highly system specific

dependant. The T7 expression system has been proved to provide a high protein expression during fermentation conditions (Lee et al., 1997).

The T7 system was developed at Brookhaven National Laboratory and is based in selectivity of the T7 RNA polymerase (Studier et al., 1990), which can be delivered to the cell from the cloned gene by induction or infection. This is a very active enzyme and elongates chains about five times faster than *E. coli* RNA polymerase. Usually the most common bacterial host strain for this expression system is *E. coli* BL21 λ DE3. These *E.coli* strain lacks the genes that code for some membrane protease that can degrade proteins during purification and the DE3 lysogene which has the transcription of the T7 RNA polymerase under the transcription control of the *lacUV5* promoter. The *lacUV5* promoter is inducible by isopropylthio- β -thiogalactoside (IPTG) which provides a tighter control of the protein expression.

2.5 Differential Scanning Calorimetry

2.5.1 Thermodynamic Background

Differential Scanning Calorimetry (DSC) is an experimental technique that has been applied to meet the contemporary demands for the quantitative and qualitative analysis of the chemical and physical phenomena in complex biological systems. This technique allows measuring the excess apparent specific heat of the system. Biological molecule in their native state are stabilized by numerous weak interactions, and generally undergoes conformational changes upon heating. Usually, the temperature range studied is of -20 to 130°C (253-403.15 K) (Chowdhry and Cole, 1989).

DSC thermogram interpretation is usually based on the following equilibrium thermodynamic equation:

$$(\delta \ln K / \delta T)_p = \Delta H_{VH} / RT^2 \quad \text{Equation 1}$$

Where K is the equilibrium constant of the process, T is the absolute temperature, ΔH_{VH} is the apparent or van't Hoff enthalpy (for a two state process), R is the gas constant (1.987 cal /mol °K) at 1 atm pressure. It is important to indicate that Equation 1 is only applicable to the two state process, also known as the all-or-none transition:

$$A \leftrightarrow B; \Delta H_{VH} = M\Delta h_{cal} = \Delta H_{cal} \quad \text{Equation 2}$$

The ΔH_{VH} in the equality above being given by the following expression

$$\Delta H_{VH} = AR(T_{1/2})^2 [C_{ex, 1/2} / \Delta h_{cal}] \quad \text{Equation 3}$$

Where M is the molecular weight of the molecule under study, Δh_{cal} is the calorimetric specific enthalpy, $T_{1/2}$ is the temperature (°C) at which the process is half completed, $C_{ex, 1/2}$ is the excess in specific heat at $T_{1/2}$, R is the gas constant and the factor A (constant based on the instrument design) has a value of 4.00. The excess specific heat is determined at constant pressure as a derivative function of the enthalpy function (Equation 4).

$$C_p = [\delta H / \delta T]_p \quad \text{Equation 4}$$

and the enthalpy function is given by equation 5, that is obtained by the integration of the heat capacity curve. The enthalpy $H(T) = \Delta H_{\text{cal}}$ is the measure of the total heat involved in the process.

$$H(T) = \int C_p(T) \delta T + H(T_0) \quad \text{Equation 5}$$

In these reactions the intermediate state between the initial and final states is not significantly populated at equilibrium. For the two-state process described, the value of $T_{1/2}$ or T_m should be independent of concentration and any equilibrium observed during an ascending temperature scan, should be exothermic.

It could be possible that in some cases $\Delta H_{\text{vH}} \neq \Delta H_{\text{cal}}$, then if $\Delta H_{\text{vH}} < \Delta H_{\text{cal}}$ this may suggest that one or more intermediates are of significance in the process and the domains change independently from each other. If $\Delta H_{\text{vH}} > \Delta H_{\text{cal}}$ intramolecular cooperation is indicated (Sturtevant, 1987).

2.5.2 Instrumentation

When a differential scanning calorimeter is used two cells: the reference cell and sample cell are filled with their respective solutions. After the injection of the reference solution and sample, heat is applied to rise their temperature between a given temperature range. Temperature changes are registered and the calorimeter supplies the system with more or less electrical power to the sample cell in order to maintain the same temperature as the reference cell (Figure 4). The differences in the thermal activity are proportional to

the difference to the heat capacity of the sample and reference in function of temperature. This data is then converted to a graphic representation, the thermogram (Plotnikov et al. 1997).

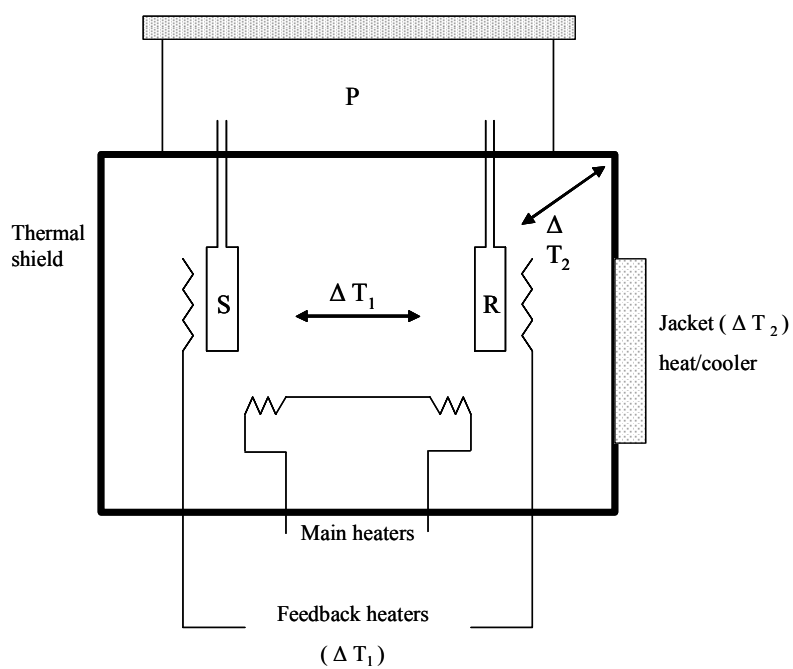


Figure 4. Diagram of a DSC used for thermal studies. The sample (S) and reference cell (R) are filled with the sample and reference respectively. During the scanning the power is supplied to the main heaters to raise the temperature, while monitoring the differences between the cells (ΔT_1) and between the cells and the jacket (ΔT_2). (Reprinted with modifications from Plotnikov et al., 1997)

3 MATERIALS AND METHODS

3.1 Recombinant Full-length Human centrin 1

The plasmid construction was made using Human centrin 1 (Hcen 1) cDNA insert of 512 bp determined by Errabolu et al. (1) and a pT7-7 vector. The pT7-7 vector is derived from the plasmid pBR322, which carry the T7 promoter (Studier et al., 1990). This recombinant was generously provided by Dr. Elmar Schiebel from Peterson Institute for Cancer Research, United Kingdom. *E. coli* BL21 λ DE3 codon plus cells from Stratagene[®] (La Jolla, CA) were transformed with Hcen 1 encoding vector (Figure 7). This *E. coli* strain carries the gene for the T7 RNA polymerase and the expression in this strain is induced by isopropylthio- β -thiogalactoside (IPTG). The vector was sent to Mayo Clinic and Foundation DNA Core Facility for sequencing and a low scale expression was performed to verify protein identity. After the low expression a blot was performed and amino acid sequencing was obtained form Mayo Clinic and Foundation Protein Core Facility.

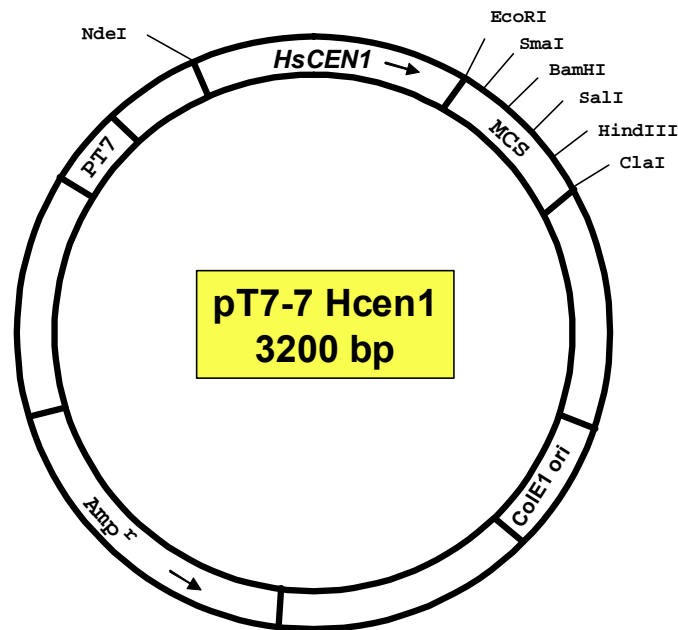


Figure 5. Map of pT7-7 vector used to express Hcen 1. The pT-7 Correspond to the T7 RNA polymerase promoter, ColE1 ori to *E.coli* origin of replication, Amp^r to ampicillin resistance and MCS to the multiple cloning site

3.2 Expression of Recombinant Protein

3.2.1 High Level Expression of Hcen 1

A transformed bacterial stock was grown in 250 mL of sterile 2xYT Broth (BIO 101, Inc., Carlsbad, CA) containing 50 µg/mL of ampicillin. Then it was incubated in an orbital shaker overnight at 37°C and 250 rpm. Twelve hours later, this culture was used to inoculate a BIOFLO 3000 fermentor vessel containing 5 L of sterile 2xYT and 50 µg/mL of ampicillin. The bacterial culture was grown at 37°C, 350 rpm of agitation, pH was continuously monitored and adjusted with 30% NH₄OH and 2.5M KH₂PO₄ to a pH of 7.0, dissolved O₂ was also monitored and adjusted and 50% glucose was added for a specified period of time during cell growth. In addition, the culture was monitored via O.D. 550 nm until it reached early log phase. The expression of Hcen 1 was then induced

with IPTG. Usually, three hours after the induction the culture reaches stationary phase and the cells are harvested by centrifugation for 30 minutes at 3,500 rpm and 4°C using a Beckman J2 MC Centrifuge with a JA-14 rotor. The pellets obtained after centrifugation were stored at -80°C for further purification. This same protocol was performed also with MARTEK 9 ¹³C labeled media (Spectra Stable Isotopes, Inc.; Columbia, MD). In the expression with the MARTEK 9 ¹³C labeled media glucose was not added during the experiment to avoid the incorporation of non labeled carbons in the expressed protein. specified period of time during cell growth. In addition, the culture was monitored via O.D. 550 nm until it reached early log phase. The expression of Hcen 1 was then induced with IPTG. Usually, three hours after the induction the culture reaches stationary phase and the cells are harvested by centrifugation for 30 minutes at 3,500 rpm and 4°C using a Beckman J2 MC Centrifuge with a JA-14 rotor. The pellets obtained after centrifugation were stored at -80°C for further purification. This same protocol was performed also with MARTEK 9 ¹³C labeled media (Spectra Stable Isotopes, Inc.; Columbia, MD). In the expression with the MARTEK 9 ¹³C labeled media glucose was not added during the experiment to avoid the incorporation of non labeled carbons in the expressed protein.

3.2.2 Biochemical Analysis

To verify the expressions levels of Hcen 1 an SDS-PAGE was performed using 15% separating and 5% stacking gel.

3.3 Protein Purification

3.3.1 Phenyl Sepharose Chromatography

For both Hcen 1 and ^{13}C -Hcen 1 The frozen cells were thawed and suspended in four times the amount (w/v) of cold lysis buffer (50 mM Tris, 0.5 mM EDTA, 0.5 M NaCl, 0.04% NaN₃ and 0.1% IGEPAL) a cocktail of protease inhibitors containing 2.0 mg/ml aprotinin, 0.5 mg/ml leupeptin and 1.0 mg/ml pepstatin A from Roche Diagnostics (Indianapolis, IN) was also added to inhibit protease degradation of the desired protein, The thawed pellet was sonicated with a macro probe while on ice 3 times x 30 second pulses at maximum power with cooling periods of one minute in ice bath. The lysate was centrifuged in a Beckman J2 MC Centrifuge with a JA-14 rotor preparative centrifuge at 10,000 rpm for 15 minutes at 4°C. The supernatant was recovered and 2 mM CaCl₂ and 4 mM Mg Cl₂ were added to it, followed by an ultracentrifugation step at 31,000 rpm for 30 minutes at 4°C using a Bekman L-80 Ultracentrifuge with a TI-80 rotor. The solution obtained on the last centrifugation was then be filtered using a low protein affinity PES membrane filter with 2 µm pore size (Nalgene[®], Rochester, NY). Once the sample was filtered affinity chromatographic procedures were performed using a Knotes 2.5cm ID x 100cm length (Vineland, NJ) loaded with Phenyl Sepharose CL-4B matrix from Sigma Aldrich Laboratories (St. Louis, MO). The equilibration buffer was 50 mM Tris, 0.5 mM EDTA, 5.0 mM EGTA, 0.5 M NaCl, 4.0 mM MgCl₂, 0.04% NaN₃, pH 7.4 and then eluted with a low calcium-containing buffer 50 mM Tris, 0.5 mM EDTA, 5.0 mM EGTA, 0.5 M NaCl, 4.0 mM MgCl₂ and 0.04% NaN₃. The column was equilibrated and run at a flow rate of 2.17 mL/min with an AUFS of 0.5 at a maximum wavelength of 280nm. The chart recorder was set at 1 cm/hour and 1 volt of sensitivity. A total of 80 fractions were

collected. The fractions were analyzed by SDS-PAGE. The protein containing fractions were pooled, concentrated, quantitated and buffer was changed for subsequent column chromatographic step. This same protocol was applied to ^{13}C labeled Hcen 1 previously over expressed.

3.3.2 Anion Exchange Chromatography

5 ml protein sample containing ~10 mg of total protein were loaded into a anion exchange column Econo-Pac High Capacity Anion-Exchange 5 mL cartridge, from Bio-Rad Laboratories (Hercules, CA). A salt gradient was prepared using (1) 50 mL of 20 mM Tris, 1 mM CaCl_2 , 1 mM DTT, 0.04% NaN_3 , pH 7.4 and (2) 50 mL of 20 mM Tris, 1 mM CaCl_2 , 1 mM DTT, 0.5 M NaCl, 0.04% NaN_3 , pH 7.4 for Hcen 1 elution. The flow rate was 2.17 mL/min with an AUFS of 0.2 at a maximum wavelength of 280nm. The chart recorder was set at 6 cm/hour and 1 volt of sensitivity. Once again, the fractions collected were analyzed by SDS-PAGE. The protein containing fractions were pooled, concentrated, quantitated and buffer was changed for subsequent lyophilization and storage.

3.3.3 Protein Characterization

SDS-PAGE was performed in order to verify purity and relative mobility. Human centrin 1 was sent to Vanderbilt University Center for Structural Biology for MALDI Mass Spectrometry to verify its molecular weight, purity and integrity. Also, a UV spectrum of the sample was taken to verify its purity based on its amino acid composition.

Molecular weight and molar extinction coefficient was calculated to be $1,309.9 \text{ cm}^{-1}\text{M}^{-1}$, based on its amino acid sequence.

3.4 Calorimetric Studies

3.4.1 Sample Preparation

After determine protein purity and integrity the protein solution was dialyzed against a buffer containing 150mM NaCl, 50mM HEPES, 4mM MgCl₂ and CaCl₂, pH 7,4 using Pirce Slide-A-Lyser[®] cassettes. Again, the sample concentration was determined using UV absorbance. Prior experimentation the sample was degassed for 5 minutes under gentle vacuum and stirring to prevent bubbles formation.

3.4.2 DSC Procedure

These experiments were done using a VP-DSC microcalorimeter by MicroCal (Northampton MA), with a cell volume of 0.50 ml, under a constant pressure of 25 psi, in order to avoid the formation of gas bubbles during the experiment. 0.50 mL of the prepared sample was injected in the sample cell with the assistance of a funnel provided by MicroCal for this purposes. The reference cell was filled in the same way with the buffer used before for dialyze the sample. Different samples of purified Hcen1 were prepared at 20 μM , 40 μM and 60 μM . The samples were degassed for at least 5 minutes prior to the experiments, using a membrane vacuum pump. The thermal perturbation was done from 10°C to 127°C with an increase of 1°C per min. The filtering period was set to 8 and the feedback mode to high. To provide maximum reproducibility of data, the thermal history of the instrument was taken into account; scans were performed with the

same start temperature and also ending temperature. The instrument was interfaced to a PC equipped with a data translation board for instrument control and automatic data collection. The excess heat capacity functions were obtained by baseline subtraction and concentration normalization. Data was processed using Origin 7, as suggested by MicroCal.

4 RESULTS AND DISCUSSION

4.1 Protein Expression and Purification

Before doing the high level expression of Hcen1, the clones provided by Dr. Elmar Schiebel, were analyzed to verify its integrity by cDNA sequencing and N-terminal amino acid sequencing. The cDNA sequencing was performed using internal primers that allow the overlay of the sequence from the insert to the vector and the sequences obtained were corroborated with the known cDNA sequence of *cen1*. Once, the clone was validated, *E.coli* BL21 λ DE 3 cells were successfully transformed with the recombinant. The expression of Hcen 1 was induced at low scale to verify protein over expression and identity. The first twelve amino acids correspond exactly to the sequence cured in the database in Hcen 1 sequence (Table 1), a remarkable detail if we consider that the amino terminal domain is the most divergent between centrin isoforms.

Table 1. Summary of Amino Acid Sequence Results for overexpressed Human centrin 1

Cycle no.	1	2	3	4	5	6	7	8	9	10	11	12	13
Human centrin 1 sequence*	M	A	S	G	F	K	K	P	S	A	A	S	T
Amino-terminal analysis	n/a**	A	S	G	F	K	K	P	S	A	A	S	T

* Experimental sequence compared with the sequence available at Expasy database, accession number Q12798. ** n/a represents non assignment for this amino acid position.

Once Hcen 1 identity was verified, a high level expression of native Hcen 1 was done. The fermentation last approximately 6 hours from inoculation to harvest. We obtained a maximum value of optical density (550 nm) of 9 and the induction point was

usually three hours after inoculation (Figure 6). From each fermentation approximately 40 grams of bacterial pellet were obtained, this pellet was frozen for further purification. For ^{13}C -labelled Hcen 1 (^{13}C -Hcen 1) the fermentation process last approximately 6 hours from inoculation to harvest and the maximum value of optical density (550 nm) obtained was of 3.75 in this case the induction point was at two hours after inoculation (Figure 7). The bacterial pellet for this experiment was 15 grams, which was also frozen for purification at a later time. An SDS-PAGE was run after each expression and an increase in protein production was observed after the induction time (Figure 8).

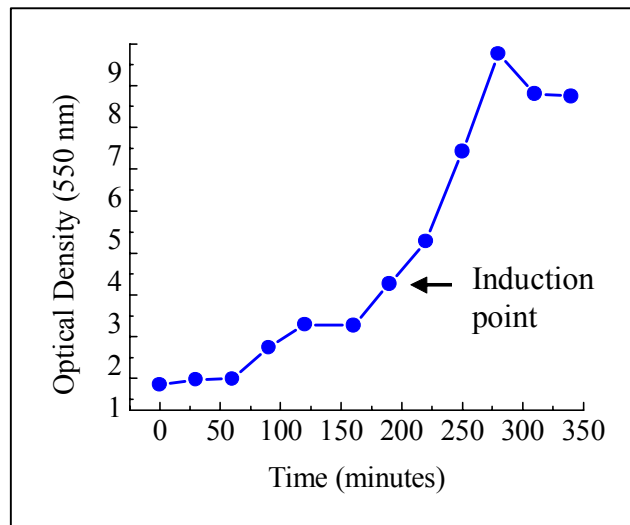


Figure 6. Growth curve for *E. Coli* transformed with pT7-7 during IPTG induction for Hcen 1 expression. The protein expression was induced at 3 hours after inoculation. The culture reaches a maximum O.D. of 9.

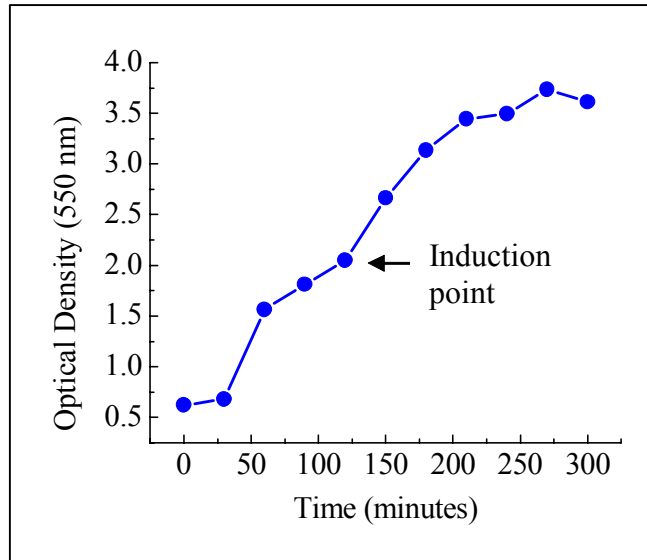


Figure 7. Growth Curve for *E. Coli* transformed with pT7-7 during IPTG induction for ¹³C- Hcen 1 labeled. The protein expression was induced at 2 hours after inoculation. The culture reaches a maximum O.D. of 3.75.

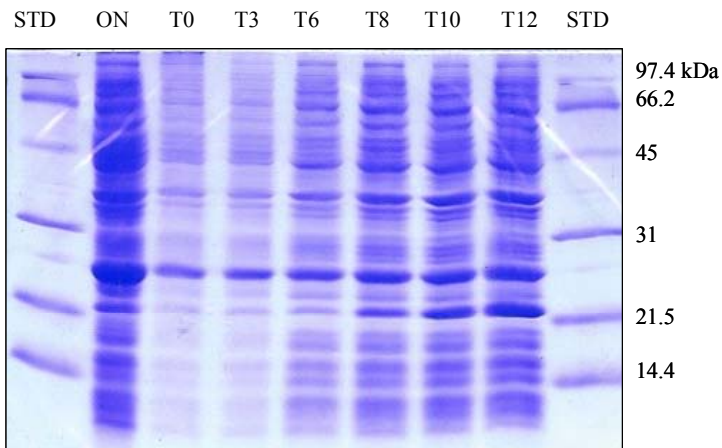


Figure 8. Time course of high level expression of Hcen 1. Lane 1 and 9: low range molecular weight standard from BioRad. Lane 2: overnight culture before the inoculation in the fermentor. Lanes 3-5: cell lysates of progressive expression during the growth curve before induction. Lanes 6-8: cell lysates of progressive expression during the growth curve after induction. The overexpression of Hcen 1 can be observed parallel to the band of the marker that corresponds to 21.5 kDa.

The results of the high level expression of Hcen 1 and ^{13}C -Hcen 1 were the expected. The growth of Hcen 1 reaches a higher O.D. measure than ^{13}C -Hcen, an indication of higher cell density. This result can be explained if we consider that the experiment was done using 2 xYT, a rich media. In contrast ^{13}C -Hcen 1 was expressed using MARTEK 9, a minimal media, that typically do not support O.D. measures higher than 3. In Figure 4.3 can be observed at ~ 20 kDa a band that correspond to Hcen 1, which increase in intensity after IPTG induction. The increasing amount of Hcen 1 expression after induction indicates that the IPTG was able to activate the transcription of T7 RNA polymerase, which in turn transcribes the Hcen1 DNA in the plasmid under the control of the T7 promoter.

For the purification process we follow the protocol established by Pastrana et al. 2002. The frozen pellet was divided into different purification batches of approximately 15 grams each to avoid overloading the column. The pellet was lysed and undergoes two centrifugation steps after being loaded in the affinity column. As we can observe in Figure 4.4, almost no protein was missing in these steps. While we can see an intense band corresponding to Hcen1 molecular weight (~ 20 kDa) in the lanes containing the supernatants (S_1 and S_2), this band is very faint in the first pellet (P_1) lane and inexistent in the second pellet (P_2) lane.

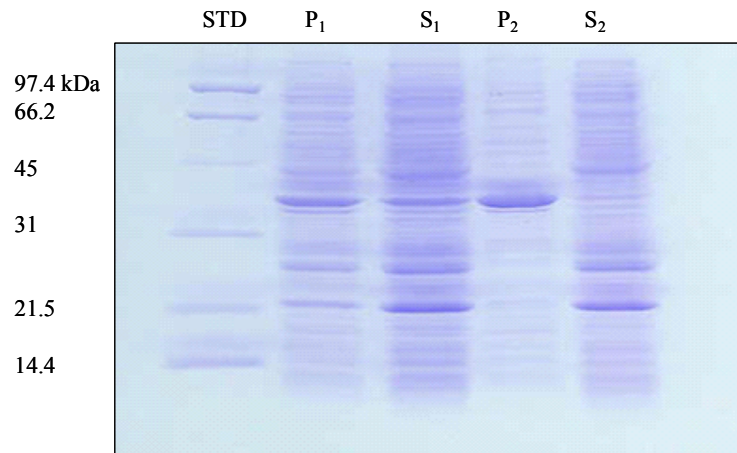


Figure 9. SDS-PAGE for the bacterial pellet lysate after high level expression. Lane 1: Low range molecular weight standard from Bio-Rad. Lane 2: bacterial pellet from the first centrifugation step (P_1). Lane 3: supernatant resulting from the first centrifugation (S_1). Lane 4: bacterial pellet from the second centrifugation step (P_2). Lane 5: supernatant resulting for the second centrifugation step (S_2), this is the final step before the sample purification.

The supernatant resulting from the last centrifugation was loaded into the affinity column. Two main peaks were obtained from the chromatogram. The first peak (A) corresponds to contaminant proteins and the second peak (B) corresponds to Hcen 1 elution (Figure 10). The protein was found in fractions from 35 to 50 (Figure 11), a decrease in protein concentration was observed as the elution progressed (Gaussian curve). These results were confirmed with a Bradford analysis, where we can observe an increase in protein concentration in fractions from 32 to 38 (Figure 12). The fractions containing Hcen 1 were pooled for the subsequent purification step. At this point of the purification process, the Hcen 1 pool was ~85% pure compared with the crude extract from the bacterial pellet lysates. These results indicate that Hcen1 binds to matrix by hydrophobic interaction and elutes once chelating agents are added.

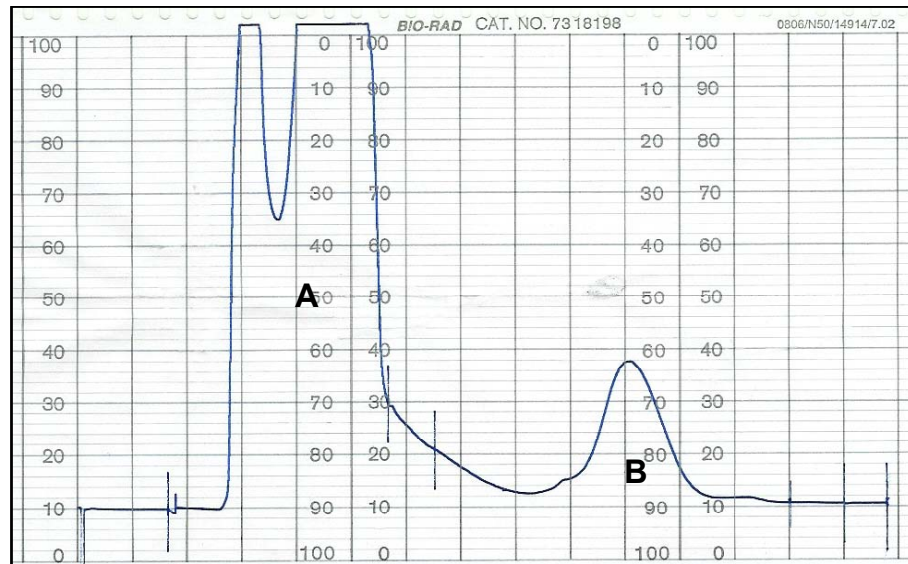


Figure 10. Elution profile characteristic of Hcen 1 through affinity chromatography. The first peak (A) represents the elution of contaminants proteins. The second peak (B) represents the elution of Hcen 1.

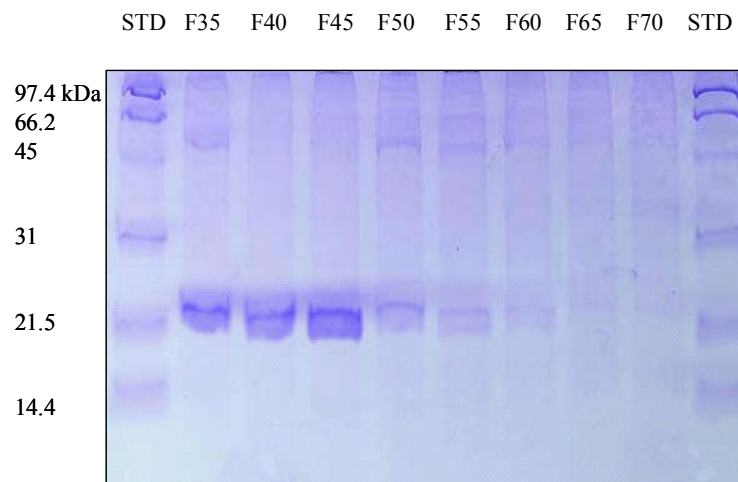


Figure 11. SDS-PAGE for the fraction eluted after affinity chromatography. Lane 1 and 10: Low range molecular weight standard from BioRad. Lane 2-8: Fractions corresponding to the second peak in the affinity column chromatogram.

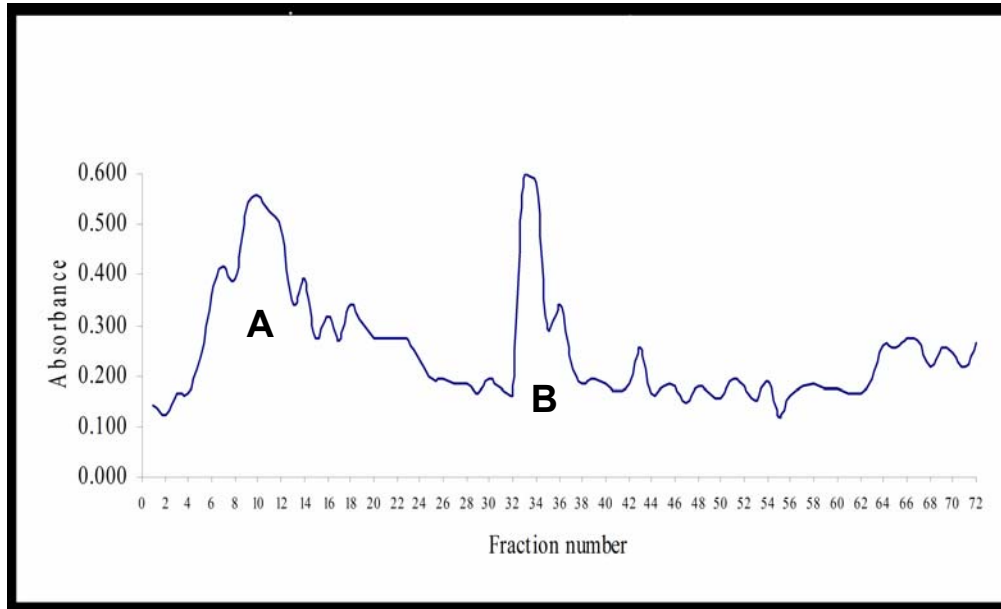


Figure 12. Bradford analysis of the fractions eluted from the affinity column. The profile obtained from the Bradford analysis agrees with the affinity column chromatogram. In both two main peaks are observed, the first corresponds to impurities and the second to Hcen 1 elution.

The pool obtained after the affinity chromatography step was loaded onto an anion exchange column. The elution profile shows three major peaks (Figure 13). The first peak (A) appears before the gradient was started and corresponds to the tubes 3 to 7. The SDS-PAGE analysis of this peak shows that some of the sample was eluted without interacting with the column; this may be due to an overloading of the column (Figure 14). These fractions were saved for future purification. The second peak (C) appears after the gradient was started and corresponds to the tubes 8 to 20. When we analyzed this peak using SDS-PAGE ~ 95% of pure Hcen 1 was obtained in tube 15, which corresponds to the peak maximum. The third peak, (D) corresponds to the tubes 23 to 36 and the analysis of the peak shows a 99% pure protein. A fourth peak appears after the buffer change (E) but the analysis of this peak does not show the presence of any protein and may be due to the change in the buffers composition. Although the protein obtained

from the second peak was 95% pure we do not pool these fractions. The 95% pure protein was filtered using a 30,000 MW centrifuge filter to eliminate the contaminant proteins.

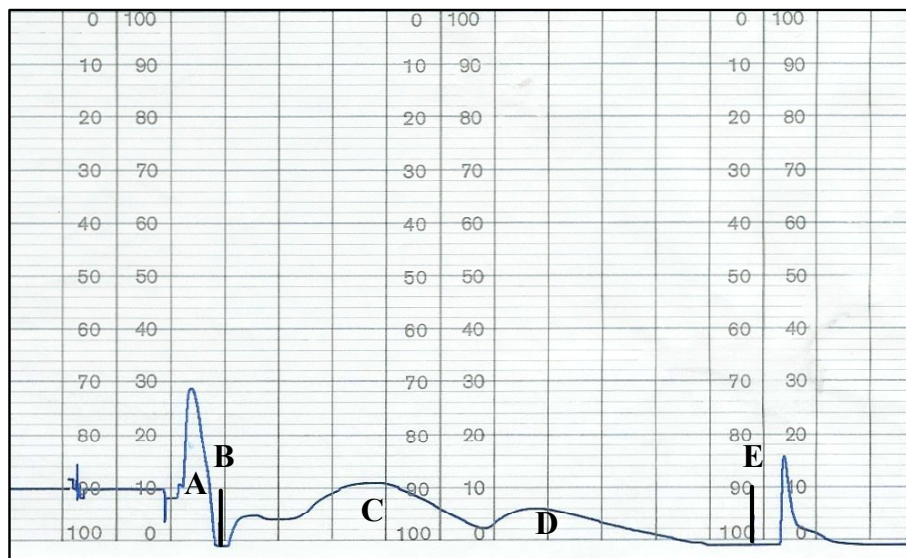


Figure 13. Elution profile characteristic of Hcen 1 through anion exchange chromatography. (A) Represents the elution of proteins that does not interact with the column. (B) Represents the initiation of the gradient. (C) Elution of the first fractions of Hcen 1, which are 95% pure. (D) Second Elution of Hcen 1, which are 99% pure. (E) Indicate the end of the gradient.

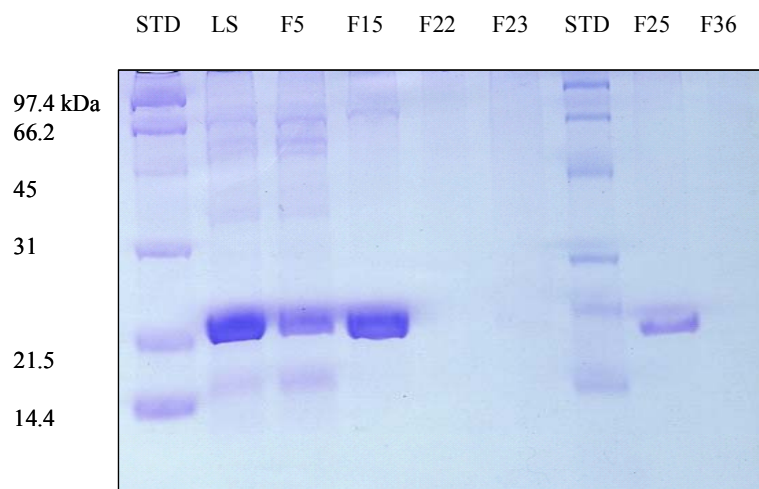


Figure 14. SDS-PAGE for the fraction eluted after affinity chromatography. Lane 1 and 7: Low range molecular weight standard from Bio-Rad. Lane 2: Sample as loaded in the column. Lane 3: Fraction corresponding to peak A in the anion exchange chromatogram. Lane 4: Fraction corresponding to peak C in the anion exchange chromatogram. Lanes 5 and 6: Fractions corresponding to the decrease and increase of peaks C and D, respectively. Lane 8: Fraction corresponding to peak D in the anion exchange chromatogram.

The pure Hcen 1 fractions obtained after anion exchange column were concentrated and their final concentration was determined by UV spectroscopy due to Hcen 1 characteristic's spectrum (Figure 15). The presence of tyrosine in the sequence is responsible for the appearance of a distinct shoulder between 284 and 264 nm and three peaks corresponding to the phenylalanine shows at 252, 258 and 264 nm. Also a MALDI mass spectroscopy analysis was done to verify its molecular weight. For Hcen 1 the results obtained are: a single peak at 19,770 m/z (Figure 16). This weight differs by ~ 200 Da from the calculated protein molecular weight but this difference might be due the calcium atoms bound which can add 40.08 Da per protein. For ^{13}C -Hcen 1 the signal peak appears at 20,559 m/z (Figure 17). In this case, an increase of the molecular weight

was ~ 849 m/z from the original weight was expected in Hcen 1 due to the isotope labeling.

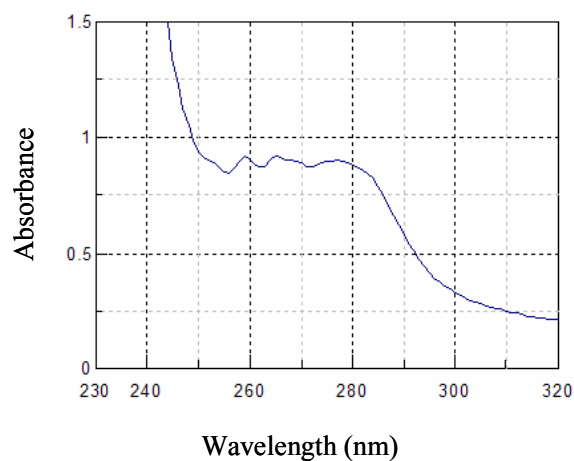


Figure 15. Characteristic UV spectra for Hcen 1. The presence of phenylalanine in the sequence is responsible for the appearance of three peaks at 252, 258 and 264 nm and the tyrosine is responsible for the characteristic shoulder between 284 and 264 nm.

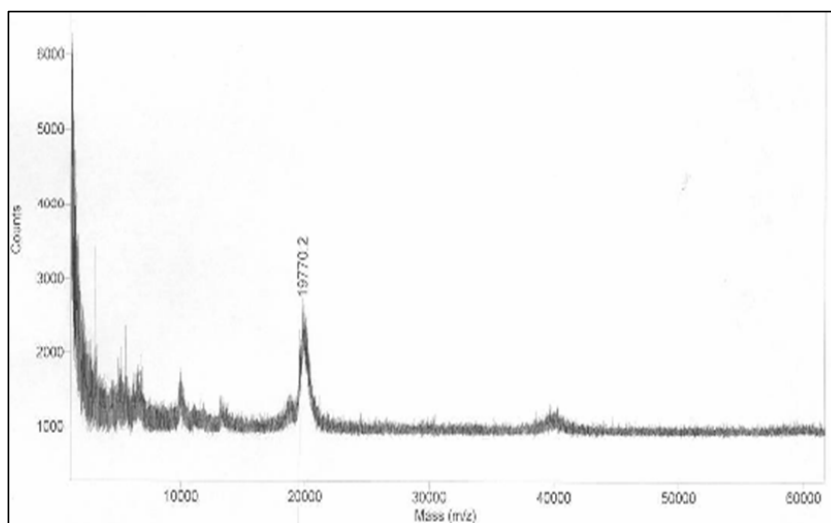


Figure 16. MALDI Mass spec for Hcen 1 after purification process. The peak obtained corresponds to 19,770 m/z which is the approximate weight of Hcen 1.

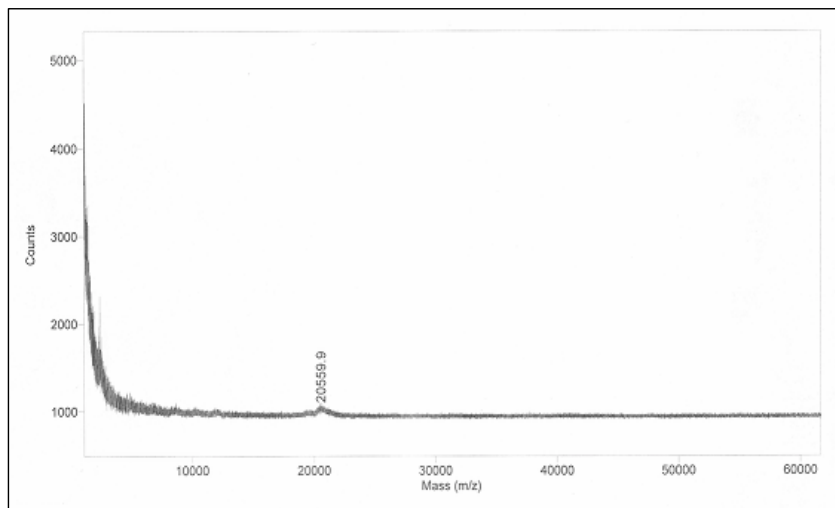


Figure 17. MALDI Mass spec for ^{13}C - Hcen 1 after purification process. The peak obtained corresponds to 20, 559 m/z which is the approximate weight of ^{13}C - Hcen 1.

4.2 Differential Scanning Calorimetry

DSC experiments were done with samples of Hcen 1 prepared at three different concentrations. Two pre-transitions peaks were observed for the sample at the three different concentrations. These two peaks can be referred to as the first pre-transition peak, for the one observed at lower temperature ($\sim 58.42^\circ\text{C}$), and the second pre-transition peak for the one observed at higher temperature ($\sim 88.82^\circ\text{C}$). In the sample at $20\ \mu\text{M}$ the first pre-transition peak is observed at 58.47°C and the second pre-transition peak at 89.53°C (Figure 18). For the sample prepared at $40\ \mu\text{M}$ the temperatures were 59.49°C for the first pre-transition peak and 88.47°C for the second pre-transition peak (Figure 19). The sample at $60\ \mu\text{M}$ presents the first pre-transition peak at 57.30°C and the second pre-transition peak at 87.57°C (Figure 20). For the three samples an abrupt

decrease in the thermogram when the temperature reached approximately 100°C and a post-transitional baseline is absent.

The lack of post-transition baseline and the appearance of negative “peak” suggesting aggregation does not allow for the proper data analysis. In addition, the appearance of the two pre-transition peaks suggests that the denaturation process of this calcium binding protein is not a two state process, thus the van’t Hoff enthalpy does not apply in this case. The calorimetric enthalpy (ΔH_{cal}) and van’t Hoff enthalpy (H_{VH}) can not be calculated. This behavior has been observed in other calcium binding proteins, as Calcium- and integrin binding protein (CIB) (Yamniuk et al. 2004) and has been related to protein aggregation. Even when conclusive thermodynamics parameters can not be determined, the transitions observed in thermogram may be related with conformational changes in Hcen 1 structure.

Previous studies demonstrated that *Chlamydomonas* centrin (Ccen) undergoes conformational changes under thermal perturbation, where its α helical content decrease (Pastrana-Rios et al., 2002). Also, is known that in Ccen its N-terminal domain has a low affinity for calcium in comparison with its C-terminal (Matei et al., 2003). These changes previously observed could explain the transitions observed in Hcen 1. The first peak could be due to the conformational change in the N- terminal domain related with its low affinity for calcium and suggest that in this first pre-transition where the calcium coordination in the terminal is affected. The second peak could represent the conformational change in the more stable C-terminal domain in respect with the calcium binding.

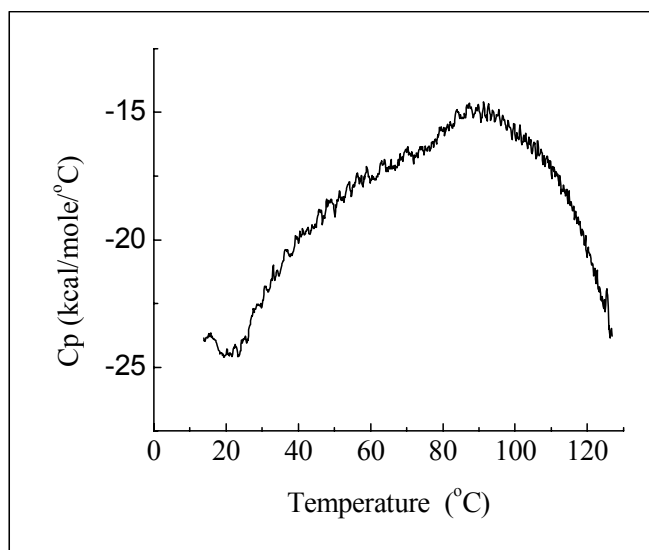


Figure 18. Thermogram for Hcen1 at 20 μM . The first pre-transition peak is observed at 58.47 $^{\circ}\text{C}$ and the second pre-transition peak at 89.53 $^{\circ}\text{C}$

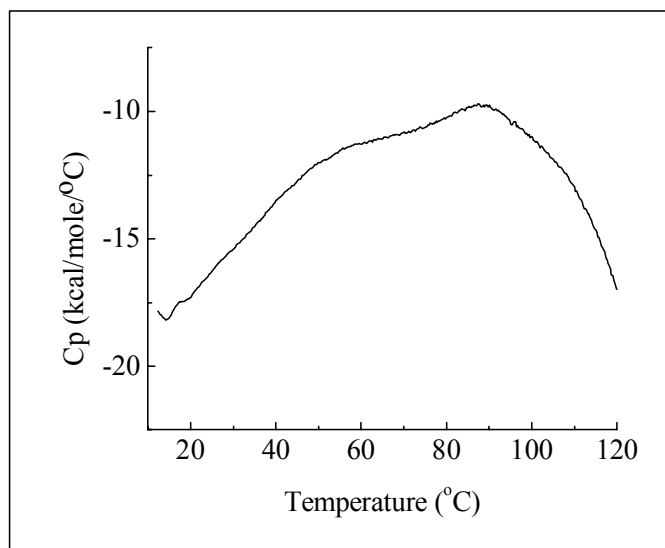


Figure 19. Thermogram of Hcen1 at 40 μM . The first pre-transition peak is observed at 59.49 $^{\circ}\text{C}$ and the second pre-transition peak at 88.47 $^{\circ}\text{C}$

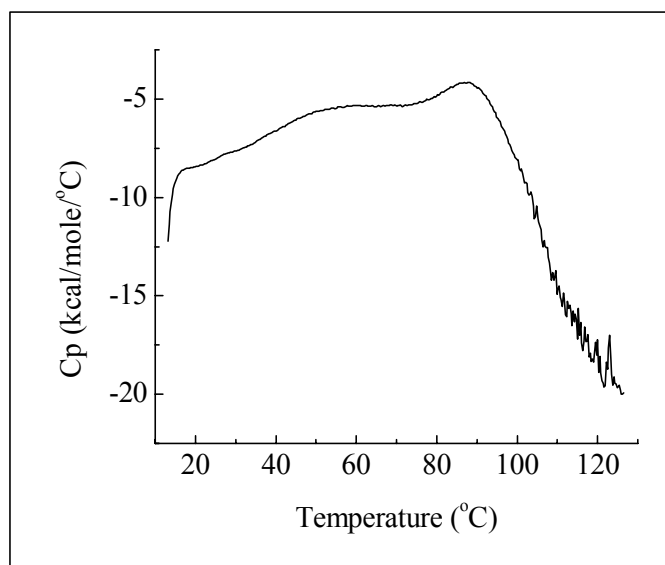


Figure 20. Thermogram of Hcen1 at 60 μ M. The first pre-transition peak is observed at 57.30 $^{\circ}$ C and the second pre-transition peak at 87.57 $^{\circ}$ C

5 CONCLUSIONS AND FUTURE WORK

The recombinant clone for the expression of Hcen 1 was effectively transformed using *E. coli* BL21 λ DE3. The high level expression of Hcen 1 was achieved, obtaining high yield of bacterial pellet used for subsequent protein purification. The purification protocol previous described for Ccen was effectively applied to Hcen 1; protein purity and identity was confirmed with amino acid sequencing and mass spectrometry analyses. The purified Hcen 1 was studied using Differential Scanning Calorimetry and the data obtained suggest that conformational changes could occurred in Hcen 1 due to the differences in the N- terminal and C- terminal domains in respect with the affinity for calcium binding.

Future investigations with Hcen 1, N-terminal domain and C- terminal domain peptides using Differential Scanning Calorimetry could help to establish the relationship within the conformational changes observed in the protein and its structure. Infrared Spectroscopy and Cicular Dicroism studies of Hcen 1 could also help to determine the effects of the conformational changes observed in Hcen 1 during the Differential Scanning Calorimetry experiments and correlated the results with the data available of the homologous proteins; Ccen and Hcen 2.

LITERATURE CITED

Baron, A. T., R. Errabolu, J. Dinusson, and J. L. Salisbury. 1995. Centrin- Based Contractile Fibers: Chromatographic Purification of Centrin. *Methods in Cell Biology*. 47: 341-351.

Bhattacharya, D., J. Steinkotter and M. Melkonian. 1993. Molecular cloning and evolutionary analysis of the calcium-modulated contractile protein, centrin, in green algae and land plants. *Plant Mol Biol*. 23: 1243-54.

Carroll, P. E., M. Okuda, H. F. Horn, P. Biddinger, P. J. Stambrook, L. L. Gleich, Y. Q. Li, P. Tarapore and K. Fukasawa. 1999. Centrosome hyperamplification in human cancer: Chromosome instability induced by p53 mutation and/or Mdm2 overexpression. *Oncogene*. 18:1935-1944.

Chang, P. and T. Stearns. 2000. δ -tubulin and ϵ -tubulin: Two new humans centrosomal tubulins reveal new aspects of centrosome structure and function. *Nat. Cell Biol*. 2:30-35.

D'Assoro, A. B., R. Busby, K. Suino, E. Delva, G. J. Almodovar-Mercado, H. Johnson, C. Folk, D. J. Farrugia, V. Vasile, F. Stivala, and J. L. Salisbury. 2004. Genotoxic stress leads to centrosome amplification in breast cancer cell lines that have an inactive G1/S cell cycle checkpoint. *Oncogene*. 23: 4068-75.

Errabolu, R., M. A. Sanders, J. L. Salisbury. 1994 Cloning of a cDNA encoding human centrin, an EF-hand protein of centrosomes and mitotic spindle poles. *J. Cell Sci*. 107: 9-16

Finst, R. J., P. J. Kim and L. M. Quarmby. 1998. Genetics of the Deflagellation Pathway in *Chlamydomonas*. *Genetics*. 149: 927-936.

Hart, P. E., J. N. Glantz, J. D. Orth, G. M. Poynter and J. L. Salisbury. 1999. Testis-Specific Murine Centrin, *Cetn1*: Genomic Characterization and Evidence for Retrotransposition of a Gene Encoding a Centrosome Protein. *Genomics*. 60: 111-120.

Henikoff, S., Greene, E. A., Pietrokovski, S., Bork, P., Attwood, T.K., and Hood, L. 1997. Gene families: The taxonomy of protein paralogs and chimeras. *Science* 278: 609–614.

- Kalt A. and M. Schliwa M. 1993. Molecular components of the centrosome. Trends Cell Biol. 3: 118-28.
- Kuboniwa, H., N. Tjandra, S. Grzesiek, H. Ren, C. B. Klee and A. Bax. 1995. Solution structure of calcium-free calmodulin. Nat. Struct. Biol. 2: 768–776.
- Lee, C., W-J Sun, B. W. Burgess, B. H. Junker, B. C. Buckland and R. L. Greasham. 1997. Process optimization for large-scale production of TGF- α -PE40 in recombinant *Escherichia coli*:effect of medium composition and induction timing on protein expression. J. Ind. Micro and Biotech. 18: 260-266.
- Lee, V. D. and B. Huang. 1993. Molecular cloning and centrosomal localization of human caltractin. Proc. Natl. Acad. Sci. 90: 11039-43.
- Lingle, W. L., Lutz, W. H., Ingle, J. N., Maihle, N. J. and Salisbury, J. L. 1998. Centrosome hypertrophy in human breast tumors: Implication for genetic stability and cell polarity. Proc. Natl. Acad. Sci. 95: 2950-2955.
- Lutz, W., W. L. Lingle, D. McCormick, T. M. Greenwood and J. L. Salisbury. 2001. Phosphorylation of Centrin during the Cell Cycle and Its Role in Centriole Separation Preceding Centrosome Duplication. J. Biol. Chem. 276: 20774-20780.
- Matei, E., S. Miron, Y. Blouquit, P. Duchambon, I. Durussel, J. A. Cox and C. T. Craescu. 2003. C-terminal half of human centrin 2 behaves like a regulatory EF-hand domain. Biochemistry. 42: 1439-50.
- Manandhar, G, C. Simerly, J. L. Salisbury and GSchatten G. 1999. Centriole and centrin degeneration during mouse spermiogenesis. Cell Motil Cytoskeleton. 43: 137-44.
- Moudjou, M., M. Paintrand, B. Vignes and M. Bornens. 1991. A human centrosomal protein is immunologically related to basal body-associated proteins from lower eucaryotes and is involved in the nucleation of microtubules. J Cell Biol. 115: 129-40.

Oakley, C.E. and B. R. Oakley. 1989. Identification of gamma-tubulin, a new member of the tubulin superfamily encoded by mipA gene of *Aspergillus nidulans*. *Nature*.;338(6217):662-4

Ortiz, M., Z. Sanoguet, H. Hu, W. J. Chaizin, C. McMurray, J. L. Salisbury and B. Pastrana-Rios. 2005. Dynamics of Hydrogen-Deuterium Exchange in *Chlamydomonas Centrin*. *Biochemistry*. 44: 2409-2418.

Palermo, G. D., L. T. Colombero and Z. Rosenwaks Z. Related Articles, Links 1997. The human sperm centrosome is responsible for normal syngamy and early embryonic development. *Rev Reprod*. 2: 19-27.

Pastrana-Rios, B., W. Ocaña, M. Rios, G. L. Vargas., G. Ysa, G. Pointer, G., J. Tapia and J. L. Salisbury. 2002. Centrin: Its Secondary Structure in the Presence and Absence of Cations. *Biochemistry*. 41: 6911-6919.

Piel, M., P. Meyer, A. Khodjakov, C. L. Reider and M. Bornes 2000. The respective contributions of the mother and daughter centrioles to the centrosome activity and behavior in vertebrate cells. *J. Cell Biol*. 149: 317-330.

Plotnikov V.V., J. M. Brandts, L. N. Lin and J. F. Brandts JF. 1997. A new ultrasensitive scanning calorimeter. *Anal Biochem*. 250: 237-44.

Salisbury, J. L., A. Baron, B. Surek, M. Melkonian. 1984. Striated flagellar roots: isolation and partial characterization of a calcium-modulated contractile organelle. *J Cell Biol*. 99: 962-70.

Salisbury, J. L. 1995. Centrin, centrosomes, and mitotic spindle poles. *Current Opinion in Cell Biology*. 7: 39-45.

Salisbury, J. L. 1998. Root. *J Eukaryot Microbiol*. 45: 28-32. Review.

Salisbury, J. L. 2001. The Contribution of Epigenetic Changes to Abnormal Centrosomes and Genomic Instability in Breast Cancer. *Journal of Mammary Gland Biology and Neoplasia*. 6: 203-212.

Sanders, M. A. and J. L. Salisbury. 1989. Centrin-mediated Microtubule Severing Flagellar Excision in *Chlamydomonas reinhardtii*. *J.Cell Biol*. 108: 1751-1760.

Sathananthan, A. H., I. Kola, J. Osborne, A. Trounson, S. C. Ng, A. Bongso and S. S. Ratnam. 1991. Centrioles in the beginning of human development. Proc Natl Acad Sci U S A. 88: 4806-10.

Sathananthan, A. H., S. S. Ratnam, S. C. Ng, J. J. Tarin, L. Gianaroli and A. Trounson. 1996. The sperm centriole: its inheritance, replication and perpetuation in early human embryos. Hum Reprod. 11: 345-56.

Schatten G. 1994. The centrosome and its mode of inheritance: the reduction of the centrosome during gametogenesis and its restoration during fertilization. Dev. Biol. 165: 299-335.

Schiebel, E., and M. Bornens. 1995. In search of a function for centrins. Trends Cell Biol. 5: 197-201.

Studier, F. W., A. H. Rosenberg, J. J. Dunn, J. W. And Dubendorff JW. 1990. Use of T7 RNA polymerase to direct expression of cloned genes. Methods Enzymol. 185: 60-89.
Sturtevant J. M. 1987. Biochemical applications of differential scanning calorimetry. Ann. Rev. Phys. Chem. 38: 463-88.

Spang, A., I. Courtney, U. Fackler, M. Matzner and E. Schiebel E. 1993. The calcium-binding protein cell division cycle 31 of *Saccharomyces cerevisiae* is a component of the half bridge of the spindle pole body. J Cell Biol. 123: 405-16.

Weich, H., B. M. Geier, T. Paschke, A. Spang, K. Grein, J. Steinkötter, M. Melkonian and E. Schiebel. 1996. Characterization of Green Algae, Yeast, and Human Centrins. J. Biol. Chem. 271: 22453-22461.

Wood, M. J. and E. A. Komovies. 1999. Production of large quantities of isotopically labeled protein in *Pichia pastoris* by fermentation. J of Biomolecular NMR. 13: 149-159.

Yamniuk, A. P., L. T. Nguyen, T. T. Hoang and H. J. Vogel. 2004. Metal ion binding properties and conformational states of calcium- and integrin-binding protein. Biochemistry. 43: 2558-68.

APPENDIX A

PRELIMINARY STUDIES OF THE EFFECT OF TAMOXIFEN IN BREAST CANCER CELL LINE MCF-7

Methods general description:

Cell lines:

Human breast cancer cell line MCF-7 was obtained from ATCC (Manassas, VA) and maintain in EMEM medium containing 5mM glutamine, 1% penicillin/streptomycin, 10% FBS and 20 µg of insulin/mL. The starvation media contains RPMI (with glutamine, without phenol red) and 5% of FBS.

Tamoxifen treatment:

The cells were plate at a density of 3×10^5 and after 48 hours the cells were treated with tamoxifen. Cell cycles regulators were added to the medium after the treatment with tamoxifen.

Cell cycle profile:

For flourescence activated cell sorting (FACS) analysis, cells were washed with cold PBS, fixed in 95% ethanol, stained with propidium iodide for 30 minutes and analyzed by flow cytometry. The NIH image J program was used for the quantitative analysis of centrosome size.

Western blotting:

For Western blot analysis, 20 µg of whole cell lysate protein were run in a 12% SDS-PAGE, transferred to PVDF membrane and fixed using 0.25% of glutaraldehyde, blocked

with 5% of nonfat milk and incubate with primary antibodies against the following proteins: phosphor retinoblastoma (as control), p53, p21, cyclin A, B, D and E, aurora A, Plk1, Plk2 and total centrin. After washing in Tween-20 buffer, PVDF membranes were incubated with MRP secondary antibodies and a signal was detected using ECL-plus reagent.

Results:

Cell cycle profile:

According with the FACS analysis at 48 hours later of the plate of the cells in the starvation media approximately 90% of the cells were in G₀/G₁ phase (Figure 1). Once the cell cycle regulators were added to the media, after 4 hours, an increase in the centrosome duplication can be seen. This centrosome duplication continues until 12 hours after the addition of the regulators, this agrees with the initiation of the S phase. At the S phase the centrosome duplication should be completed prior to the initiation of mitosis. This confirms that untreated MCF-7 cells have a couple cell and centrosomes cycles even when treated with tamoxifen.

Western blotting:

The comparison of MCF-7 starved cells and MCF-7starved/treated with Tamoxifen cells shows a delayed on cyclins E and D, while cyclins A and B appeared at the same time in both treated and untreated cells (Figure 2). The expression of centrin was also verified and was constant in tamoxifen treated cells. These results may suggest that tamoxifen is

causing cell cycle deregulation that is overcome due to the expression of cyclins A and B and that the cell cycle is uncoupled with the centrosome cycle. The uncoupling between the two cycles may cause centrosome duplication that can lead to chromosome instability even in cells treated with chemotherapeutic drugs.

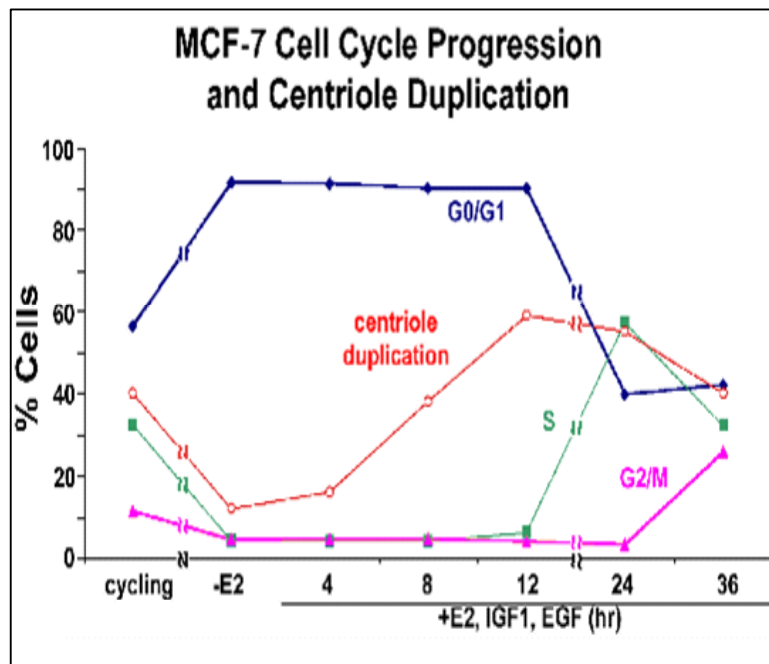


Figure 1. Fluorescence activated cell sorting (FACS) analysis for MCF-7 cells and quantitative analysis for centrosome size and number. This analysis shows the relation between cell cycle progression and centriole duplication.

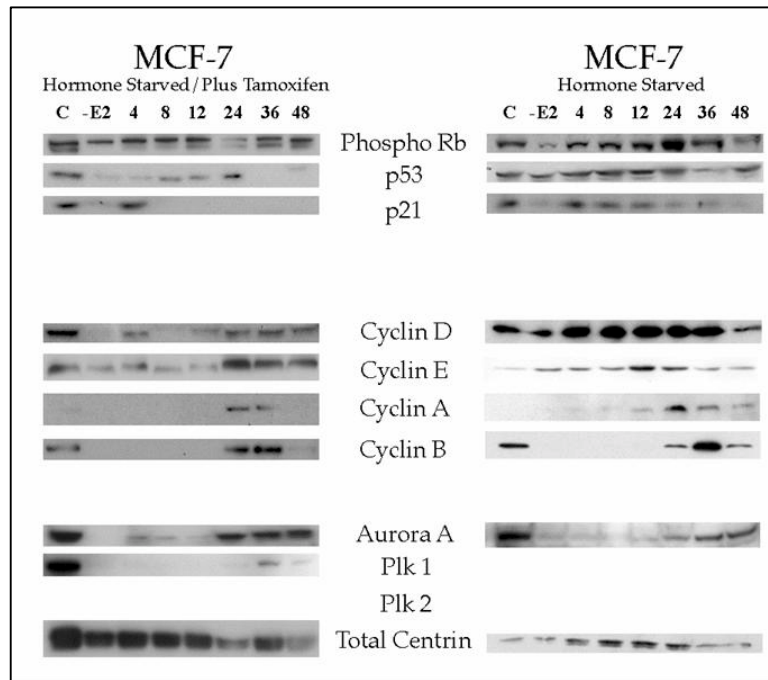


Figure 2. Comparison of cell cycle regulator proteins among MCF-7 starved cells and MCF-7starved/treated cells.